JOC Article

4′-Substituted-4-biphenylyloxenium Ions: Reactivity and Selectivity in Aqueous Solution

Michael Novak,*,† Matthew J. Poturalski,† Whitney L. Johnson,† Matthew P. Jones,† Yueting Wang,† and Stephen A. Glover§

Department of Chemistry and Biochemistry, Miami University, Oxford, Ohio 45056, and School of Biological, Biomedical, and Molecular Sciences, Division of Chemistry, University of New England, Armidale, 2351, New South Wales, Australia

novakm@muohio.edu.

Received January 30, 2006

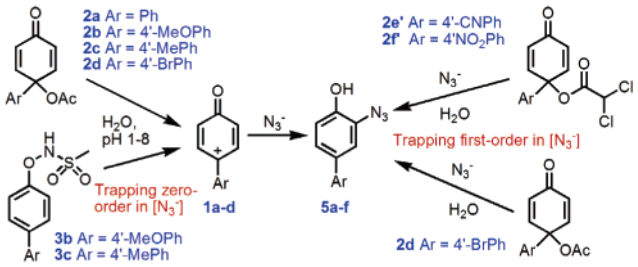

Azide trapping shows that the 4′-substituted-4-biphenylyloxenium ions **1b**−**d** are generated during hydrolysis of 4-aryl-4-acetoxy-2,5-cyclohexadienones, **2c** and **2d**, and *O*-(4-aryl)phenyl-*N*-methanesulfonylhydroxylamines, **3b** and **3c**. In addition, the 4′-bromo-substituted ester, **2d**, undergoes a kinetically second-order reaction with N_3^- that accounts for a fraction of the azide adduct, **5d**. Since both first-order and second-order azide trapping occurs simultaneously in **2d**, the second-order reaction is not enforced by the short lifetime of **1d**, which has similar azide/solvent selectivity to the unsubstituted ion, **1a**. In contrast the 4′-CN and 4′-NO_2 ions **1e** and **1f** cannot be detected by azide trapping during the hydrolysis of the dichloroacetic acid esters **2e′** and **2f′** even though ^{18}O labeling experiments show that a fraction of the hydrolysis of both esters occurs through C_{alkyl}−O bond cleavage. These esters exhibit only second-order trapping by azide. Correlations of the azide/solvent selectivities of **1a**−**d** with the calculated relative driving force for hydration of the ions (ΔE of eq 4) determined at the pBP/DN*//HF/6-31G* and BP/6-31G*//HF/6-31G* levels of theory suggest that **1e** and **1f** have lifetimes in the 1−100 ps range. Ions with these short lifetimes are not in diffusional equilibrium with nonsolvent nucleophiles, and must be trapped by such nucleophiles via a preassociation mechanism. The second-order trapping that is observed in these two cases is enforced by the short lifetime of the cations, and may occur by a concerted S_N2' mechanism or by internal azide trapping of an ion sandwich produced by azide-assisted ionization. Comparison of azide/solvent selectivities of the oxenium ions **1a**−**c** with the corresponding biphenylylnitrenium ions **8a**−**c** shows that 4′-substituent effects on reactivity in both sets of ions are similar in magnitude, although the nitrenium ions are ca. 30-fold more stable in an aqueous environment than the corresponding oxenium ions. The magnitude of the 4′-substituent effects for electron-donating substituents suggest that both sets of ions are more accurately described as 4-aryl-1-imino-2,5-cyclohexadienyl or 4-aryl-1-oxo-2,5-cyclohexadienyl carbocations. Calculated structures of the oxenium ions are also consistent with this interpretation.

Introduction

Aryloxenium ions, **1**, are often invoked as intermediates in oxidation reactions of phenols, including many reactions that are synthetically useful.[1−3] Although there are known examples of isolatable or slowly reacting oxenium ions, including the oxenium ion derived from α-tocopherol,[4−6] it is not clear that transient oxenium ion intermediates are formed in all the

* Address correspondence to this author.
† Miami University.
§ University of New England.

(1) Swenton, J. S.; Carpenter, K.; Chen, Y.; Kerns, M. L.; Morrow, G. W. *J. Org. Chem.* **1993**, *58*, 3308−3316. Swenton, J. S.; Callinan, A.; Chen, Y.; Rohde, J. L.; Kerns, M. L.; Morrow, G. L. *J. Org. Chem.* **1996**, *61*, 1267−1274.

10.1021/jo060198r CCC: $33.50
Published on Web 04/19/2006

SCHEME 1

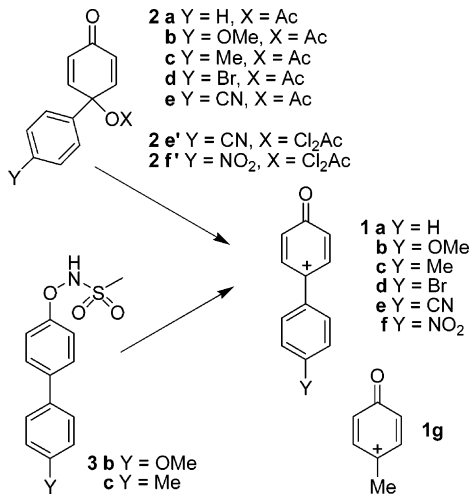

proposed cases. Since most of the synthetic examples were carried out in solvent mixtures containing nucleophilic protic solvents such as H_2O, MeOH, and carboxylic acids, and the effects of substituents on cation stability are not known, it is possible that the proposed ions are too short-lived to exist as intermediates under these conditions. Alternative reaction mechanisms would then be enforced by the lack of an intermediate with a finite lifetime.[7] We have previously shown that the 4-biphenylyloxenium ion, **1a**, does have sufficient lifetime in aqueous solution to be trapped by nonsolvent nucleophiles, but the 4-methylphenyloxenium ion, **1g**, could not be detected under similar reaction conditions.[8,9] The apparent oxenium ion reaction products derived from precursors of **1g** are formed via a kinetically bimolecular process that may be enforced by the short lifetime of **1g**.[9,10]

We have expanded our study of aryloxenium ions to include the attempted generation of 4′-substituted-4-biphenylyloxenium ions **1b**−**f** to examine a series of ions with an expected wide range of aqueous solution lifetimes. Our motivation was to determine the nature of substituent effects on ion reactivity/selectivity, reaction products, and the possible onset of bimolecular mechanisms enforced by short lifetimes for a series of ions with similar structural and steric features. Potential precursors to these ions under solvolytic conditions include 4-aryl-4-carboxy-2,5-cyclohexadienones, **2**, and *O*-(4-aryl)phenyl-*N*-methanesulfonylhydroxylamines, **3** (Scheme 1). Both types of precursors have been utilized previously, although evidence that the hydroxylamine precursors yield oxenium ions has been circumstantial.[8,9,11,12] In this paper we report azide trapping of **1b**−**d** generated from either **2** or **3** and the onset of a bimolecular substitution reaction apparently enforced by the short lifetimes of **1e** and **1f** in H_2O. The lifetimes of the ions **1a**−**d**, determined by the "azide clock" procedure,[7,13] correlate well with the relative stabilities of these ions to hydration calculated at the pBP/DN*//HF/6-31G* and BP/6-31G*//HF/6-31G* levels of theory. These calculations predict aqueous solution lifetimes for **1e** and **1f** that are in the picosecond range. The results of this study are of general interest because aryloxenium ions are isoelectronic with the much better characterized arylcarbenium and nitrenium ions, and we compare the observed and calculated properties of **1a**−**f** with those of analogous nitrenium species herein.

Results and Discussion

The precursors **2c**−**e** were synthesized by standard methods already described for **2a**.[8] The MeO-substituted compound **2b** was not isolated because the attempted oxidation of 4′-methoxy-4-biphenylol by phenyl iodonium diacetate (PIDA) in AcOH led only to polymeric material. Because **2e** proved to be unreactive, the dichloroacetic acid esters **2e′** and **2f′** were synthesized by methods outlined previously.[9] The sulfonamides **3b** and **3c** were made by adaptation of published procedures.[12,14,15] All compounds were stable enough to be purified by recrystallization or chromatography on silica gel. Synthesis and characterization of all compounds is presented in the Supporting Information.

Kinetics of decomposition of **2**, **2′**, and **3** were measured at 30 °C in 5 vol % CH_3CN-H_2O at $\mu = 0.5$ ($NaClO_4$) in $HClO_4$ solutions (pH <3.0), or in $HCO_2H/NaHCO_2$, AcOH/AcONa, Na_2HPO_4/NaH_2PO_4, and $TrisH^+$/Tris buffers by monitoring changes in UV absorbance as a function of time. Absorbance vs time data fit a first-order or consecutive first-order rate equation well. Consecutive first-order reactions were found only for **3b** at pH <2.5. Under these conditions one rate constant was found to be experimentally equivalent to the rate constant for acid catalyzed rearrangement of authentic **4b**, the only observable initial product of decomposition of **3b** under these conditions (see below). This reaction was not examined further. Buffer effects were found to be minimal with the exception of **2c** and **2d** which exhibited common ion rate depression in acetate buffers similar to that previously observed for **2a**.[8] Most rate data in buffer solutions were obtained at total buffer concentrations of 0.02 M and were not corrected by extrapolation to 0 M buffer. Rate constants taken at a minimum of two wavelengths were averaged for each compound at each pH. The pH dependence of the reactions is summarized in Figures 1 and 2. The acetic acid esters **2c** and **2d** exhibit pH dependence of decomposition qualitatively identical with that previously

(2) Rieker, A.; Beisswenger, R.; Regier, K. *Tetrahedron* **1991**, *47*, 645−654. Rodrigues, J. A. R.; Abramovitch, R. A.; de Sousa, J. D. F.; Leiva, G. C. *J. Org. Chem.* **2004**, *69*, 2920−2928. Baesjou, P. J.; Driessen, W. L.; Challa, G.; Reedjik, J. *J. Am. Chem. Soc.* **1997**, *119*, 12590−12594. Driessen, W. L.; Baesjou, P. J.; Bol, J. E.; Kooijman, H.; Spek, A. L.; Reedjik, J. *Inorg. Chim. Acta* **2001**, *324*, 16−20. Kobayashi, S.; Higashimura, H. *Prog. Polym. Sci*. **2003**, *28*, 1015−1048.
(3) Pelter, A.; Ward, R. S. *Tetrahedron* **2001**, *57*, 273−282.
(4) Rieker, A.; Speiser, B.; Straub, H. *DECHEMA Monogr.* **1992**, *125*, 777−782.
(5) Dimroth, K.; Umbach, W.; Thomas, H. *Chem. Ber*. **1967**, *100*, 132−141.
(6) Williams, L. L.; Webster, R. D. *J. Am. Chem. Soc.* **2004**, *126*, 12441−12450. Lee, S. B.; Lin, C. Y.; Gill, P. M.; Webster, R. D. *J. Org. Chem.* **2005**, *70*, 10466−10473.
(7) Jencks, W. P. *Acc. Chem. Res.* **1980**, *13*, 161−169.
(8) Novak, M.; Glover, S. A. *J. Am. Chem. Soc.* **2004**, *126*, 7748−7749.
(9) Novak, M.; Glover, S. A. *J. Am. Chem. Soc.* **2005**, *127*, 8090−8097.
(10) Glover, S. A.; Novak, M. *Can. J. Chem.* **2005**, *83*, 1372−1381.
(11) Abramovitch, R. A.; Inbasekaran, M.; Kato, S. *J. Am. Chem. Soc.* **1973**, *95*, 5428−5430. Abramovitch, R. A.; Alvernhe, G.; Bartnik, R.; Dassanayake, N. L.; Inbasekaran, M. N.; Kato, S. *J. Am. Chem. Soc*. **1981**, *103*, 4558−4565. Uto, K.; Miyazawa, E.; Ito, K.; Sakamoto, T.; Kikugawa, Y. *Heterocycles* **1998**, *48*, 2593−2600.
(12) Endo, Y.; Shudo, K.; Okamoto, T. *J. Am. Chem. Soc.* **1977**, *99*, 7721−7723. Endo, Y.; Shudo, K.; Okamoto, T. *J. Am. Chem. Soc.* **1982**, *104*, 6393−6397.
(13) Richard, J. P.; Jencks, W. P. *J. Am. Chem. Soc*. **1982**, *104*, 4689−4691; **1982**, *104*, 4691−4692; **1984**, *106*, 1383−1396.
(14) (a) Sakurai, H.; Tsukada, T.; Hirao, T. *J. Org. Chem.* **2002**, *67*, 2721−2722. (b) Krause, J. G. *Synthesis* **1972**, 140.
(15) Endo, Y.; Shudo, K.: Okamoto, T. *Synthesis* **1980**, 461−463.

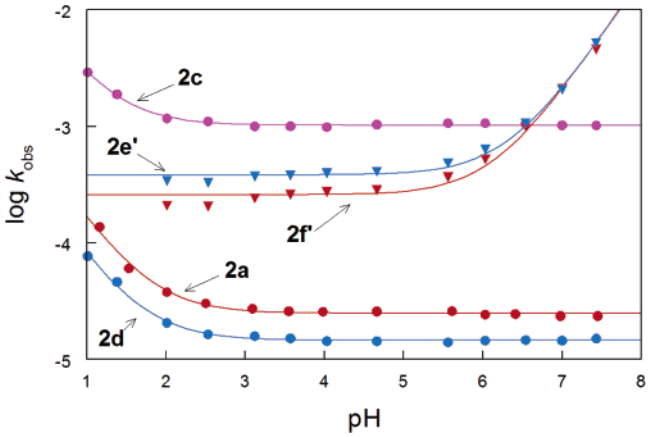

FIGURE 1. pH dependence of the decomposition of **2a**, **2c**, **2d**, **2e′**, and **2f′** at 30 °C. Data for **2a** are from ref 8. Rate constants reported in Table 1 are from the least-squares fits illustrated in the figure.

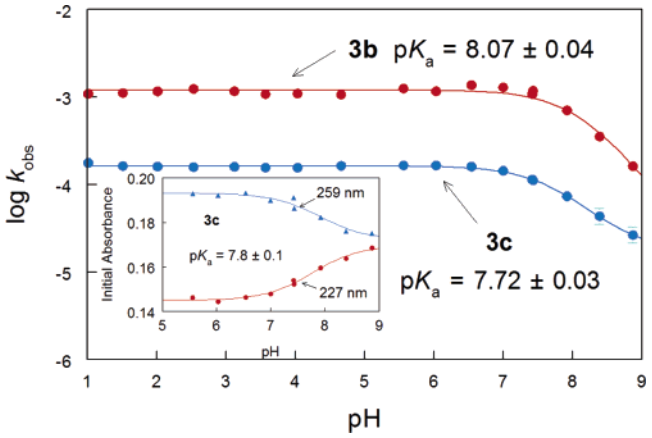

FIGURE 2. pH dependence of the decomposition of **3b** and **3c** at 30 °C. The lines are least-squares fits of the data to eq 1 as described in the text. Derived rate parameters are reported in Table 1. Insert: Spectrophotometric titration of **3c** at 227 and 259 nm.

reported for **2a** with two observable rate constants k_o and k_H,[8] while **2e′** and **2f′** show behavior reminiscent of **2g′** with rate

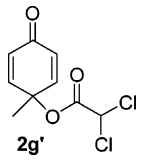

constants k_o and k_{OH}.[9] The rate constants k_H and k_{OH} describe H_3O^+-dependent and OH^--dependent decomposition pathways, respectively, while k_o describes a pH-independent decomposition that is significant for all esters over a wide pH range. Rate constants are reported in Table 1. The decomposition of **2e** was exceedingly slow. No significant changes in UV absorbance were detected over a 2-day period and HPLC experiments confirmed less than 5% decomposition of a sample in a pH 7.0 buffer incubated at 30 °C for 1 week.

Compounds similar to **3b** and **3c** are known to require addition of TFA or TFSA to decompose in benzene,[11] so we were surprised to observe that both of these sulfonamides exhibited facile pH-independent decomposition from pH 1 to 7 with no evidence of acid-catalyzed decomposition (Figure 2). At pH >7.0 there is a decrease in the rate of decomposition of both esters associated with an apparent ionization of the substrate. Titration of **3c** confirmed that the kinetic pK_a does correspond to an observed spectrophotometric pK_a (Figure 2, insert). Kinetic data in Figure 2 were fit to eq 1. Within the pH range examined there is no evidence for decomposition of ionized **3b**, so the second term of eq 1 was not used in that fit. The complete equation was used for **3c** since there is detectable decomposition of its conjugate base. Derived rate constants are summarized in Table 1. The decomposition reactions at pH > pK_a were not examined further.

$$k_{obs} = ([H^+]/(K_a + [H^+]))k_o + (K_a/(K_a + [H^+]))k_- \quad (1)$$

The decomposition products observed by HPLC for all compounds in the absence of strong nonsolvent nucleophiles at pH 2.5, 4.6, and 7.0 are the 4-aryl-4-hydroxy-2,5-cyclohexadienones, **4**. Identities were confirmed by comparison to

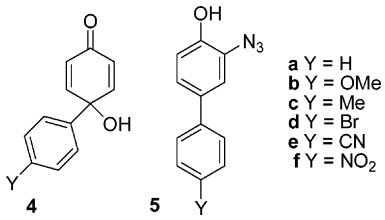

authentic samples, and yields determined by HPLC were 90−100% in all cases except **4b**. This quinol was generated quantitatively from **3b** at pH 2.5, but in ca. 50% yield at pH 4.6, and ca. 25% at pH 7.0. Although the yield of **4b** was pH dependent, it was not dependent on buffer concentration in the range 0.005−0.020 M. All quinols were stable in aqueous solution for at least 5 half-lives of the corresponding precursor with the exception of **4b**, which did undergo an apparent dienone−phenol rearrangement described above at noticeable rates at pH <2.5.

Results of azide trapping experiments performed on **2c** and **2d** are summarized in Figure 3. In both cases an azide adduct **5c** or **5d** is generated at the expense of the quinol **4c** or **4d** as

TABLE 1. Derived Rate Parameters for the Decomposition of 2a, 2c, 2d, 2e′, 2f′, 3b and 3c[a]

compd	k_o (s^{-1})	k_H ($M^{-1}\,s^{-1}$)	$10^{-5}k_{OH}$ ($M^{-1}\,s^{-1}$)	pK_a	10^5k_- (s^{-1})
2a[b]	(2.50 ± 0.05) × 10^{-5}	(1.45 ± 0.08) × 10^{-3}			
2c	(1.02 ± 0.01) × 10^{-3}	(1.95 ± 0.08) × 10^{-2}			
2d	(1.46 ± 0.02) × 10^{-5}	(6.80 ± 0.24) × 10^{-4}			
2e′	(3.8 ± 0.1) × 10^{-4}		1.8 ± 0.1		
2f′	(2.6 ± 0.1) × 10^{-4}		1.9 ± 0.2		
3b	(1.20 ± 0.04) × 10^{-3}			8.07 ± 0.04	
3c	(1.64 ± 0.02) × 10^{-4}			7.72 ± 0.03	1.7 ± 0.1

[a] Conditions: 30 °C, μ = 0.5 ($NaClO_4$), parameters reported with their estimated standard deviations obtained from the least-squares fits. [b] Data from ref 8.

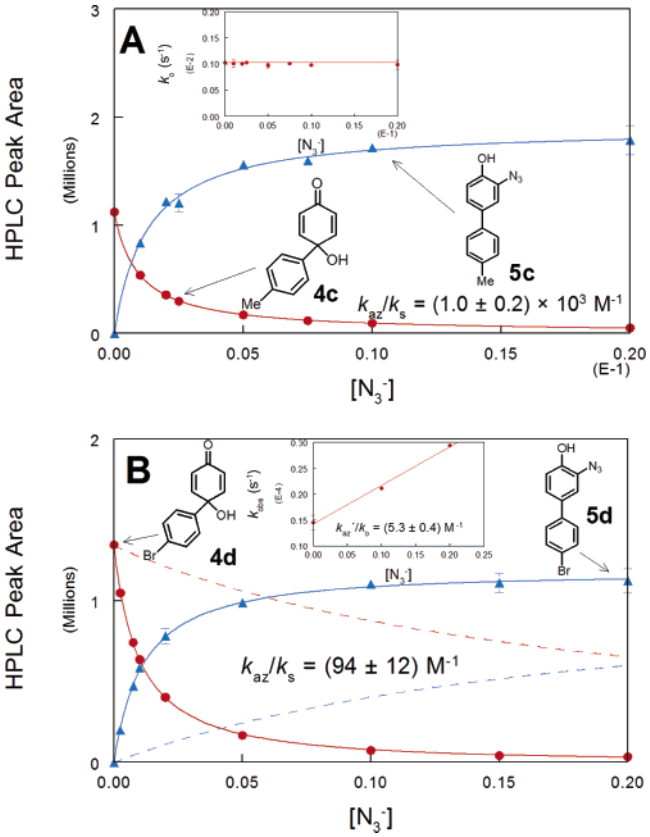

FIGURE 3. Azide trapping experiments for **2c** (A) and **2d** (B) performed at pH 7.0 in 0.02 M phosphate buffer. Data were fit by least-squares procedures to the standard "azide clock" equations[7,13] for **2c** or to eqs 2 and 3 for **2d**. The dashed lines in Figure 3B show the amount of trapping that can be attributed to the kinetically bimolecular process governed by k_{az}' (Scheme 2). Inserts: Rate constants for decomposition of **2c** and **2d** in the presence of N_3^-.

$[N_3^-]$ increases. For **2c**, trapping by N_3^- occurs with no acceleration of its rate of decomposition (Figure 3A, insert). All of **5c** can be attributed to trapping of the cation **1c**. Fitting of the product data to the standard "azide clock" equations[7,13] generates k_{az}/k_s, the ratio of the second-order rate constant for trapping of the cation by N_3^- to the first-order rate constant for trapping by the aqueous solvent. Data in Table 2 show that **1c** reacts with N_3^- considerably more selectively than does **1a**. The common ion effect, k_{OAc}/k_s, tabulated in Table 2 is also somewhat larger for **1c**, but qualitatively **1c** reacts very similarly to **1a**.[8]

SCHEME 2

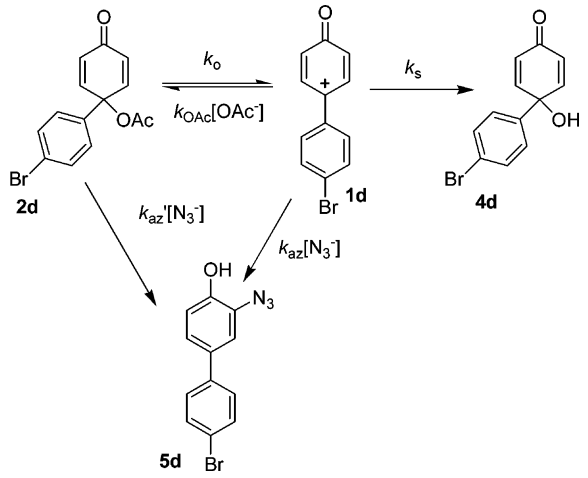

The situation for **2d** is more complicated. N_3^- accelerates the decomposition reaction (Figure 3B, insert). The rate constant ratio k_{az}'/k_o that expresses the acceleration by N_3^- is small (Table 2), but not negligible. The second-order reaction of **2d** with N_3^- could either generate **5d** by a substitution process on the quinoid ring or generate **4d** by nucleophilic acceleration of ester hydrolysis. The yield of **4d** reaches an asymptote of 0 at high $[N_3^-]$. This indicates that the latter process does not occur. The second-order reaction must yield **5d**, but Figure 3 shows that this reaction is not efficient enough to account for all the observed yield of **5d**. The common ion rate depression observed for **2d** indicates that a dissociative process occurs for this ester. If the data are interpreted in terms of the mechanism of Scheme 2, the product yields for **4d** and **5d** can be fit to eqs 2 and 3 ($[\mathbf{4d}]_o$ is the yield of **4d** in the absence of N_3^-, $[\mathbf{5d}]_\infty$ is the yield of **5d** at infinite $[N_3^-]$) to determine k_{az}/k_s for **1d**. In these fits k_{az}'/k_o was given the value obtained from the kinetic data. All other variables were treated as adjustable least-squares parameters. The results of those calculations are shown in Figure 3B and in Table 2. The cation **1d** is about as selective toward N_3^- as is **1a**.

$$[\mathbf{4d}] = [\mathbf{4d}]_o(1/(1 + k_{az}'[N_3^-]/k_o))(1/(1 + k_{az}[N_3^-]/k_s)) \quad (2)$$

$$[\mathbf{5d}] = [\mathbf{5d}]_\infty((k_{az}'[N_3^-]/k_o) + (k_{az}[N_3^-]/k_s)/(1 + k_{az}[N_3^-]/k_s))(1 + k_{az}'[N_3^-]/k_o) \quad (3)$$

TABLE 2. Rate Constant Ratios from Azide Trapping and Common Ion Effect, and Δ*E* of Eq 4[a]

compd	k_{az}/k_s (M^{-1})	k_{az}'/k_o (M^{-1})	k_{OAc}/k_s (M^{-1})	$1/k_s$ (ns)[b]	Δ*E* (kcal/mol)[c]
2a	77 ± 5		3.3 ± 0.2	12 ± 1	0 (0)
2c	(1.0 ± 0.2) × 10^3		7.0 ± 0.5	150 ± 30	3.41 (5.46)
2d	94 ± 12	5.3 ± 0.4	5.0 ± 0.3	14 ± 3	1.26 (0.66)
2e′		184 ± 3[d]			−10.90 (−9.39)
		195 ± 10[e]			
2f′		237 ± 5[d]			−14.00 (−12.74)
		256 ± 14[e]			
3b	(1.2 ± 0.1) × 10^5			(1.8 ± 0.2) × 10^4	11.45 (13.12)
3c	(1.2 ± 0.1) × 10^3			180 ± 20	3.41 (5.46)

[a] Conditions: 30 °C, μ = 0.5 ($NaClO_4$), kinetic parameters are reported with their estimated standard deviations. [b] Calculated assuming k_{az} = 6.5 × 10^9 M^{-1} s^{-1}.[8] [c] Calculated at the pBP/DN*//HF/6-31G* level[8–10] or (in parentheses) BP/6-31G*//HF/6-31G* level. [d] Determined from the slope and intercept of k_{obs} vs $[N_3^-]$ data. [e] Determined by application of "azide clock" equations to product data.

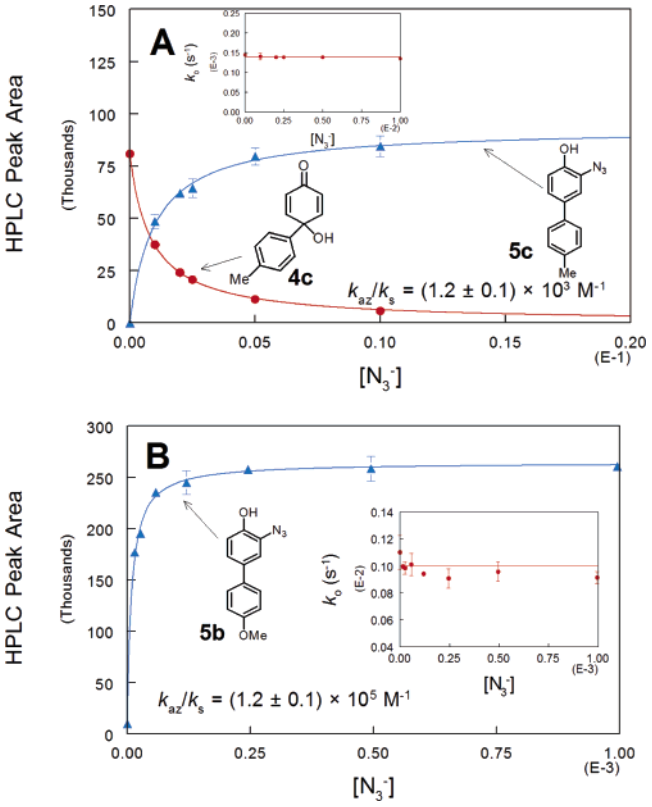

FIGURE 4. Azide trapping experiments for **3c** (A) and **3b** (B) performed at pH 7.0 in 0.02 M phosphate buffer. Data were fit by least-squares procedures to the standard "azide clock" equations.[7,13] Inserts: Rate constants for decomposition of **3c** and **3b** in the presence of N_3^-.

The bimolecular substitution governed by k_{az}' for **2d** is not enforced by the short lifetime of **1d**. This cation has an estimated lifetime of 14 ns if k_{az} is diffusion limited at 6.5×10^9 M^{-1} s^{-1}.[8] This is a sufficient lifetime for the species to exist as a "free" ion in solution so that a preassociation mechanism is not required to account for its trapping.[7] The ion **1a** has a similar calculated lifetime of 12 ns and its precursor **2a** does not exhibit observable second-order decomposition reactions in solutions containing N_3^- at similar concentrations to those employed here.[8] The more strongly inductively electron withdrawing 4-(4′-bromophenyl) substituent of **2d** may favor the bimolecular substitution that competes with oxenium ion formation in this compound.

The sulfonamide **3c** decomposes into the quinol **4c** with yields of 90−100% throughout the pH range of the pH-independent decomposition. Azide trapping at pH 7.0 generated **5c** without rate acceleration (Figure 4A). The k_{az}/k_s ratio determined from the product yield data was indistinguishable from that obtained for **2c** (Table 2). Both **2c** and **3c** generate the same intermediate identified as **1c**. In both cases the reaction proceeds without significant competing side reactions as judged by quantitative yields of **4c** in the absence of nonsolvent nucleophiles and quantitative yields of **5c** at high $[N_3^-]$.

Although **3b** does not generate **4b** in quantitative yield in phosphate buffer at pH 7.0, addition of N_3^- to this buffer does generate 90−100% yields of **5b** at $[N_3^-] > 1$ mM. Azide trapping occurs without rate acceleration and is very selective (Figure 4B and Table 2). At pH 2.5 at which **4b** is generated

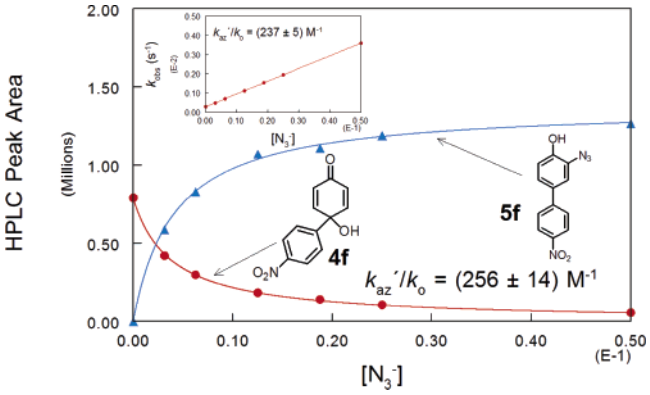

FIGURE 5. Azide trapping experiments for **2f′** performed at pH 4.6. Data were fit by least-squares procedures to the standard "azide clock" equations.[7,13] Insert: Rate constants for the decomposition of **2f′** in the presence of N_3^-.

quantitatively, Br^- also traps **1b** to generate the bromide adduct **6b**, although with much less selectivity than N_3^-: k_{Br}/k_s =

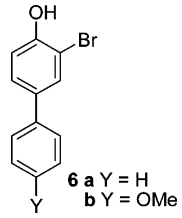

$(2.5 \pm 0.5) \times 10^2$ M^{-1}. We previously showed that Br^- traps **1a** under acidic conditions to yield the analogous product **6a**.[9] In both cases only one bromide adduct was observed.

The dichloroacetic acid esters **2e′** and **2f′** were studied because the corresponding acetic acid esters are very unreactive. Both of these compounds react in a second-order fashion with N_3^- at pH 4.6, and yield azide adducts **5e** and **5f**, respectively. The structures of these adducts were shown to be completely analogous to **5a**−**d** by HSQC and HMBC NMR experiments that allowed assignment of all ^{13}C resonances in all adducts. Rate constant ratios k_{az}'/k_o determined from kinetic and product data were equivalent within experimental error (Table 2). Data are shown for **2f′** in Figure 5. The results show that within experimental error the entire yield of the azide adducts can be accounted for by the kinetically bimolecular reaction of the esters with N_3^-. There is no evidence for trapping of an intermediate by N_3^- as observed for the other precursors. Limited experiments with **2e** also showed that this ester reacted with N_3^- to yield **5e**. The decomposition of **2e** is accelerated by N_3^- but detailed kinetic and product analyses were not performed.

Results of LC/MS analysis of the ^{18}O content of **4e** and **4f** generated from **2e′** and **2f′** in pH 4.6 0.02 M acetate buffer containing 25 atom % ^{18}O are summarized in Scheme 3. Negative ion ESI was found to be the most efficient ionization method so peaks at *m*/*e* 210 ($(M - 1)^-$) and 212 ($(M + 1)^-$) were analyzed for **4e** and the analogous peaks at *m*/*e* 230 and 232 for **4f**. Analysis was performed after 1 half-life of the decomposition reaction of **2e′** or **2f′** on **4e** or **4f** generated from ester decomposition and on control samples that contained authentic **4e** or **4f** incubated under the same conditions for the same length of time. The control experiments are meant to correct for any ^{18}O incorporation into the carbonyl O of the

SCHEME 3

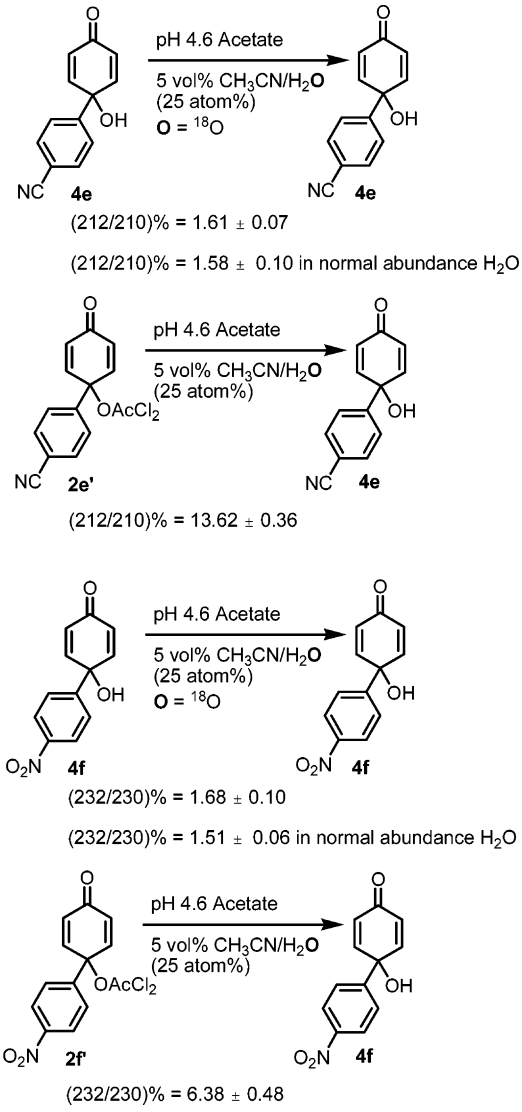

quinol, although the data show that this does not occur to a significant extent under these conditions. The results show that the predominant mode of reaction of these esters in aqueous solution at this pH is ester hydrolysis by $C_{acyl}-O$ bond cleavage, but **2e′** decomposes with (36 ± 1)% $C_{alkyl}-O$ bond cleavage calculated from (212/210)% after correction by (212/210)% in the control experiment. The same calculation for **2f′** with use of the (232/230)% data indicates (14 ± 2)% $C_{alkyl}-O$ cleavage in the decomposition of that ester.

The characteristics of the reactions of **2e′** and **2f′** are similar to those of **2g′** with the exception that no evidence for $C_{alkyl}-O$ bond cleavage could be found for **2g′** at pH 4.6.[9] An upper limit of 3% was established for this ester based on a statistical analysis of error limits of the measured ion ratios in the control experiment.[9] By contrast, **2a** undergoes decomposition entirely by $C_{alkyl}-O$ bond cleavage at pH 7.0 with generation of **1a** as determined by labeling experiments in $^{18}O-H_2O$, common ion rate depression, and azide trapping without rate acceleration that leads to no residual **4a** at high $[N_3^-]$.[8,9] Similar trapping data presented above show that **2c** and **2d** also react in aqueous solution by predominant or exclusive $C_{alkyl}-O$ bond cleavage, although there is an alternate and inefficient second-order azide trapping route for **2d**. The generation of **4b** from **3b** and **4c** from **3c**, and the azide trapping results for these compounds unambiguously show that they undergo N−O bond cleavage with generation of **1b** from **3b** and **1c** from **3c**.

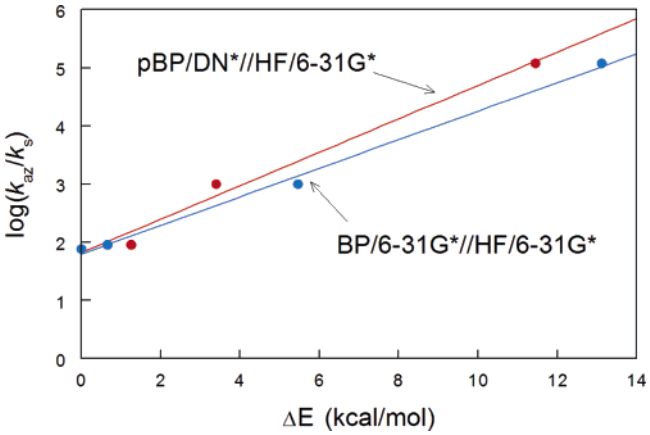

FIGURE 6. Correlation of $\log(k_{az}/k_s)$ for the ions **1a**−**d** vs ΔE of eq 4 calculated at the pBP/DN*//HF/6-31G* (red) and BP/6-31G*//HF/6-31G* (blue) levels of theory. Correlation lines are from nonweighted linear least-squares fits.

The last column of Table 2 collects calculated values for ΔE of the isodesmic reaction of eq 4 for all ions determined by

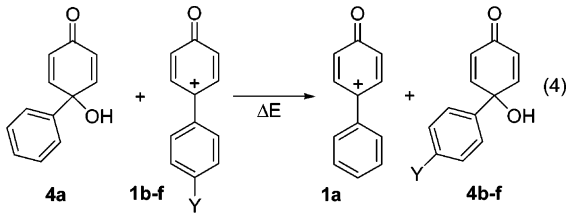

DFT methods at two levels of theory: pBP/DN*//HF/6-31G* and BP/6-31G*//HF/6-31G*. The former method has been used by us to understand and correlate the properties of **1a**, **1g**, and structurally related nitrenium ions,[8−10] and BP is a standard DFT functional used in a wide variety of applications.[16] ZPE and thermodynamic corrections were not applied because we have found that these corrections largely cancel when used in isodesmic reactions such as that shown in eq 4.[8−10,17] Equation 4 estimates the driving force for hydration of the cations **1b**−**f** relative to that of **1a**. We have used ΔE of similar isodesmic reactions to correlate the hydration kinetics of nitrenium ions.[17] Figure 6 shows a linear correlation of $\log(k_{az}/k_s)$ vs ΔE of eq 4 calculated at both levels for the ions **1a**−**d**. The correlation constant, r^2, is 0.986 for pBP/DN*//HF/6-31G* and 0.995 for BP/6-31G*//HF/6-31G*. A correlation with use of data at the B3LYP/6-31G*//HF/6-31G* level (r^2 = 0.980) was similar while the HF/6-31G* correlation (r^2 = 0.908) was less successful. Both of these methods incorrectly predict the relative hydrolytic stability of **1d** and **1a**. On the basis of analogies to directly measured k_{az} for nitrenium ions of similar reactivity, it is expected that k_{az} for **2a**−**d** is diffusion limited.[18,19] If so, Figure 6 indicates that log k_s correlates negatively with ΔE, the relative driving force for hydration of the cations. A similar conclusion has been reached for a wide range of nitrenium ions,

(16) Matyus, P.; Fuji, K.; Tanaka, K. *Tetrahedron* **1994**, *50*, 2405−2414. Abashkin, Y. G.; Collins, J. R.; Burt, S. K. *Inorg. Chem.* **2001**, *40*, 4040−4048. Abashkin, Y. G.; Burt, S. K. *Org. Lett.* **2004**, *6*, 59−62. Ciezak, J. A.; Trevino, S. F. *THEOCHEM* **2005**, *723*, 241−244.
(17) Novak, M.; Lin, J. *J. Org. Chem.* **1999**, *64*, 6032−6040.
(18) Ren, D.; McClelland, R. A. *Can. J. Chem.* **1998**, *76*, 78−84.

although the calculations were performed at a different level of theory (HF/6-31G*//HF/3-21G).[17] The correlation provides a basis for estimating the lifetimes ($1/k_s$) of the undetected ions **1e** and **1f**. Extrapolation of the two correlation lines with use of ΔE data for **2e′** and **2f′** in Table 2 provides an estimate of 7−48 ps for the lifetime of **1e** and 1−7 ps for **1f**. The longer lifetime is provided in each case by the BP/6-31G* method.

Because of accumulated errors associated with the assumptions used in the calculations, and the rather long extrapolations, these lifetime estimates are not highly reliable, but they do indicate that both **1e** and **1f** are very short-lived species bordering on transition states. It is possible that the hydrolysis reactions for both **2e′** and **2f′** that involve C_{alkyl}−O bond cleavage proceed through short-lived oxenium ions, but species with lifetimes in the 1−100 ps range cannot be efficiently trapped by nonsolvent nucleophiles. All reactions with such nucleophiles must proceed through some form of preassociation mechanism because of the short lifetime of the free cation.[7] Preassociation without assistance to ionization is inefficient and inconsistent with the observed N_3^--induced rate accelerations for decomposition of **2e′** and **2f′**.[7] The observed reaction with N_3^- must occur either through a fully concerted S_N2' mechanism or by internal azide trapping of an ion sandwich, **7**, produced

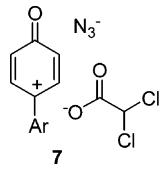

7

by azide-assisted ionization. We have previously argued that such a species has insufficient lifetime to be an intermediate in the case of **2g′** where the cation **1g** is also estimated to have a lifetime in the picosecond range.[9] If this is the case, the S_N2' mechanism is enforced. Others have argued that the fully concerted S_N2' mechanism is never observed,[20] and energetic conditions that must be met for a concerted transition state involving multiple bond-making/bond-breaking events are stringent.[21] We are planning isotope effect studies of the second-order azide trapping reaction in an effort to shed more light on this issue.

Comparisons of the reactivity patterns of **1a**−**c** and the analogous nitrenium ions **8a**−**c** are possible since Ren and McClelland generated **8a**−**c** as laser flash photolysis products

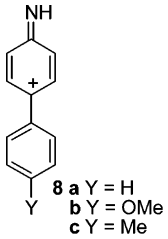

8 a Y = H
b Y = OMe
c Y = Me

of the corresponding azides in 20 vol % CH_3CN-H_2O at 20 °C.[18] Reaction conditions are similar to those used in this study so direct comparisons are worthwhile. The 4′-Me and 4′-MeO substituents stabilize both oxenium and nitrenium ions toward hydration relative to the unsubstituted ions to approximately the same extent, ca. 10-fold for the 4′-Me ions and ca. 1500-fold for the 4′-MeO ions. However, each nitrenium ion is ca. 30-fold more stable than the corresponding oxenium ion. For example, the estimated lifetime of **1b** is 0.018 μs (Table 2) while the observed lifetime of **8b** is 0.63 μs. Ren and McClelland used the magnitude of the 4′-substituent effects on k_s in **8b** and **8c**, which were significantly more stabilizing than expected from a correlation of log k_s vs σ^+ for 3′-substituted examples, to argue that 4-biphenylylnitrenium ions had a dominant benzylic cation structure illustrated by the resonance structure shown above.[18] Since the magnitude of the stabilizing effects on k_s observed in **1b** and **1c** are almost identical with those observed for **8b** and **8c**, a similar conclusion can be made for the structures of the oxenium ions. We have already noted that the calculated structure of **1a** optimized at HF/6-31G* is most consistent with that expected for the 4-aryl-1-oxo-2,5-cyclohexadienyl resonance structure used in Scheme 1.[10] In all cases the C−O bond length is short (1.187−1.189 Å) and the unscaled calculated CO stretching frequencies (ca. 2020 cm^{-1}) are slightly larger than the CO stretching frequencies for the corresponding **4** (ca. 2000 cm^{-1}). Perhaps a more sensitive measure of the cyclohexadienyl/oxenium contributions to the structures of **1a**−**f** can be found in the bond length alternations in the proximal ring of the 4-biphenylyl cations. A complete table of bond lengths in that ring for **1a**−**f** is provided in the Supporting Information. The data show significant bond length alternation of ca. 1.09−1.10 for C1−C2/C2−C3 and 1.11−1.12 for C3−C4/C2−C3, with alternation decreasing monotonically from the kinetically most stable (**1b**, 1.104, 1.117) to the least stable (**1f**, 1.090, 1.114) ion. These results suggest some increase in oxenium character for the less stable ions, but all of these species appear to be predominately carbenium in character. Nonetheless, the oxenium center does impart unique reactivity patterns to these ions that, in our opinion, justify the continued use of the term "oxenium ion" to describe these species.

This study has identified two ions, **1b** and **1c**, that have sufficiently long lifetimes to be readily observed if generated by laser flash photolysis. Efforts are now underway to generate appropriate photoprecursors to these ions.

Conclusion

Kinetically first-order azide trapping demonstrates that, like **1a**, 4′-substituted-4-biphenylyloxenium ions, **1b**−**d**, with electron-donating substituents are generated from both esters of 4-aryl-4-hydroxy-2,5-cyclohexadienones, **2**, and *O*-(4-aryl)phenyl-*N*-methanesulfonylhydroxylamines, **3**. However, oxenium ion-like substitution products can be generated via two additional pathways not involving oxenium ions. The first of these is a kinetically second-order process that occurs simultaneously with the oxenium ion process for the 4′-bromo-4-biphenylyloxenium ion **1d**. This mechanism is not enforced by the short lifetime of the ion, since trapping of the ion can be demonstrated as a competing process. For precursors with more strongly electron-withdrawing substituents (4′-CN and 4′-NO_2), the oxenium ion cannot be detected by trapping procedures, and correlations of oxenium ion lifetime with the DFT-based calculated driving force for hydration suggest that **1e** and **1f** have lifetimes in the 1−100 ps range. Ions with such short lifetimes cannot be trapped by nonsolvent nucleophiles via diffusionally controlled processes. The second-order azide trapping observed for the

(19) Davidse, P. A.; Kahley, M. J.; McClelland, R. A.; Novak, M. *J. Am. Chem. Soc.* **1994**, *116*, 4513−4514. McClelland, R. A.; Davidse, P. A.; Hadzialic, G. *J. Am. Chem. Soc.* **1995**, *117*, 4173−4174. McClelland, R. A.; Gadosy, T. A.; Ren, D. *Can. J. Chem.* **1998**, *76*, 1327−1337. Bose, R.; Ahmad, A. R.; Dicks A. P.; Novak, M.; Kayser, K. J.; McClelland, R. A. *J. Chem. Soc., Perkin Trans. 2* **1999**, 1591−1599.

(20) Bordwell, F. G. *Acc. Chem. Res.* **1970**, *3*, 281−290.

(21) Guthrie, J. P. *J. Am. Chem. Soc.* **1996**, *118*, 12878−12885.

precursors **2e′** and **2f′** is then enforced by the short lifetimes of the ions. It remains to be determined if this trapping reaction is a truly concerted S_N2' process, or an azide-assisted ionization with trapping proceeding within a short-lived ion sandwich.

Experimental Section

Synthesis. The esters **2c**−**e**, **2e′**, and **2f′** were synthesized by oxidation of the 4′-substituted-4-hydroxybiphenyls with PIDA in acetic acid or in dichloroacetic acid. The 4′-substituted-4-hydroxybiphenyls were purchased (4′-Br, 4′-CN) or made by a Suzuki coupling procedure (4′-MeO, 4′-Me) or by nitration followed by hydrolysis of 4-(benzoyloxy)biphenyl (4′-NO_2).[14a,22] Detailed procedures for the oxidation have been published elsewhere.[8,9] Crude reaction products were subjected to chromatography on a chromatatron (2 mm silica gel, 25/75 to 50/50 EtOAc/hexanes eluent). Final purification was accomplished by recrystallization from EtOAc/hexanes (**2c**−**e**, **2e′**), or further chromatography on the chromatatron (**2f′**, 50/50 EtOAc/hexanes). Characterization of each compound is presented in the Supporting Information.

The sulfonamides **3b** and **3c** were generated from the corresponding 4′-substituted-4-hydroxybiphenyls[14a] by amination of the phenoxide with *O*-mesitylenesulfonylhydroxylamine in DMF,[14b,15] followed by treatment of the resulting hydroxylamine with methanesulfonyl chloride in pyridine.[12] Details of the amination and sulfonylation procedures, as well as purification and characterization of **3b**, **3c**, and their precursors *O*-(4-(4′-methoxyphenyl)phenyl)-hydroxylamine and *O*-(4-(4′-methylphenyl)phenyl)hydroxylamine, are described in the Supporting Information.

Authentic samples of the quinols **4b**−**f** were made by oxidation of the corresponding 4-hydroxybiphenyls with PIDA in 50/50 CH_3CN/H_2O as previously described for **4a**.[8] Each quinol was purified by chromatography on a chromatatron (2 mm silical gel, 50/50 EtOAc/hexanes) followed by recrystallization from EtOAc/hexanes. Characterization is provided in the Supporting Information. An authentic sample of the bromo-adduct **6b** was made by bromination of 4-hydroxy-4′-methoxybiphenyl[14a] with bromine in $CHCl_3$.[23] The azide adducts **5b**−**f** were isolated from reaction mixtures by a method similar to that described for **5a**.[8] Briefly, The ester **2c** or **2d** or sulfonamide **3b** (0.20 mmol), dissolved in 2 mL of CH_3CN, was added in 200 μL aliquots every half-life as determined by the reaction kinetics (below) to 100 mL of a 0.02 M phosphate buffer (5 vol % CH_3CN-H_2O, pH 7.0, $\mu = 0.5$ ($NaClO_4$)) containing 0.2 M NaN_3 that was incubated in the dark at 30 °C. After the last addition, the mixture was incubated in the dark at 30 °C for an additional 10 half-lives. After cooling in an ice−water bath, the reaction mixture was extracted with CH_2Cl_2 (4 × 25 mL). After drying over Na_2SO_4, the extract was evaporated to dryness and the residue was purified by chromatography on a chromatatron (2 mm silica gel, CH_2Cl_2 eluent). A similar procedure was followed for **2e′** and **2f′** except that 100 mL of a 0.2 M azide buffer (5 vol % CH_3CN-H_2O, pH 4.6, $\mu = 0.5$ ($NaClO_4$)) was utilized as the reaction medium. Characterization of the azide adducts is provided in the Supporting Information.

Kinetics and Product Analysis. Detailed procedures for the preparation of solutions and monitoring kinetics by UV spectroscopy or HPLC are provided elsewhere.[8,9] Stock solutions of most compounds were prepared at ca. 0.01 M in CH_3CN to obtain initial concentrations of 5×10^{-5} M in the reaction solutions after injection of 15 μL of the stock solution into 3 mL of the aqueous reaction solution. The sulfonamides **2b** and **2c** precipitated under these conditions, so 0.002 M solutions of these compounds in CH_3CN were prepared to obtain 1×10^{-5} M concentrations in the reaction medium. All reactions followed by UV spectroscopy were monitored at a minimum of two wavelengths, and rate constants obtained at each wavelength were averaged. Product yields were monitored by HPLC on the same solutions used for kinetics. HPLC conditions were the following: 20 μL injections on a 4.7 mm × 250 mm C-8 column, 60/40 $MeOH/H_2O$ eluent, 1.0 mL/min flow rate, UV detection at 240 nm. Procedures for fitting product yield data to the standard "azide clock" equations have been published.[9] Similar procedures were used to fit the product data for **4d** and **5d** to eqs 2 and 3, respectively.

^{18}O Labeling Experiments. Details for preparing solutions are found elsewhere.[9] A 2.5 μL volume of a 0.02 M solution of **4e** or **4f** or a 0.04 M solution of **2e′** or **2f′** in CH_3CN was injected into 500 μL of a 25 atom % pH 4.6 acetate buffer preincubated at 30 °C. After 1 half-life of the hydrolysis reaction (1800 s for **4e** and **2e′**, 2700 s for **4f** and **2f′**) the reaction mixture was cooled in an ice−water bath and analyzed by LC/MS, using triplicate injections. LC conditions were the following: 4.6 mm × 250 mm C-8 column, 60/40 $MeOH/H_2O$ (0.1% HOAc), 1 mL/min, 20 μL injection, retention time for **4e** ca. 4.2 min, and for **4f** ca. 5 min. Control experiments for **4e** and **4f** in normal isotopic distribution reaction solutions were also performed. Mass spectra were obtained on an ion trap instrument. The electrospray ionization source (ESI) was operated in negative mode with enhanced resolution to achieve total baseline separation of isotopic peaks. The capillary, skimmer 1, and trap drive voltages were 3500, −22.1, and 37.7 V, respectively. Ion charge control was on with a target of 30 000. The 350 °C nitrogen dry gas flow rate was 12 L/min and the nebulization gas pressure was 60 psi. Each point of the total ion current (TIC) chromatogram consisted of an average of 8 scans over a mass range of m/z 50−350. The mass spectra used for quantitation consisted of an average of three to five points of the extracted ion chromatogram (EIC) beginning at the apex of the peak. These points were chosen to have the best signal-to-noise ratio and resolution. Automatic generation of the mass list, intensities, and areas was used except for the M + 2 isotope of the control sample spectra, which was integrated manually. The M + 4 isotopic peaks were not discernible above the baseline noise.

Calculations. Extensive descriptions of calculation methods applied to **1a** and **4a** have been published.[10] The same procedures were followed for **1b**−**f** and **4b**−**f** utilizing Spartan 04 for Macintosh Version 1.0.1 and Spartan Version 5.[25] Geometries were optimized at the HF/6-31G* level. Frequency analyses were performed at this level to verify that all geometries corresponded to true stationary points. These geometries were used to obtain energies at the perturbative Becke−Perdew density functional level pBP/DN*//HF/6-31G*.[26] Calculations were also carried out at the BP/6-31G*//HF/6-31G*[26] level, which is implemented in Spartan 04 and at the B3LYP/6-31G*//HF/6-31G* level. Optimized HF/6-31G* geometries and energies at all levels calculated are presented in the Supporting Information.

Acknowledgment. The authors thank the donors of the Petroleum Research Fund for support of this research (Grant No. 43176-AC4). The 500 MHz NMR spectrometer and the LC/MS were provided by grants to MU by the Hayes Investment Fund of the Ohio Board of Regents.

Supporting Information Available: Characterization of **2c**−**e**, **2e′**, **2f′**, **4b**−**f**, **5b**−**f**, and **6b**, synthesis and characterization of **3b** and **3c**, optimized geometries (HF/6-31G*) for **1b**−**f** and **4b**−**f**, comparison of selected HF/6-31G* bond lengths in **1a**−**f**, and ^{13}C NMR spectra of **2c**−**e**, **2e′**, **2f′**, **4b**−**f**, **5b**−**f**, and **6b**. This material is available free of charge via the Internet at http://pubs.acs.org.

JO060198R

(22) Ou, S. H.; Percec, V.; Mann, J. A.; Lando, J. B.; Zhou, L.; Singer, K. D. *Macromolecules* **1993**, *26*, 7263−7273.
(23) Gutsche, C. D.; No, K. H. *J. Org. Chem.* **1982**, *47*, 2708−2712.
(24) Novak, M.; Kahley, M. J.; Eiger, E.; Helmick, J. S.; Peters, H. E. *J. Am. Chem. Soc*. **1993**, *115*, 9453−9460.
(25) Wavefunction, Inc.; 18401 Van Karman Ave., Suite 370, Irvine, CA, 92612.
(26) Becke, A. D. *Phys. Rev. A* **1988**, *38*, 3098−3100. Perdew, J. P. *Phys. Rev. B* **1986**, *33*, 8822−8824.